NeuroImage: Clinical 36 (2022) 103256

Contents lists available at ScienceDirect

NeuroImage: Clinical

journal homepage: www.elsevier.com/locate/ynicl

Increased functional connectivity between nucleus basalis of Meynert and amygdala in cognitively intact elderly along the Alzheimer's continuum

Qingze Zeng [a,1], Tiantian Qiu [b,1], Kaicheng Li [a,1], Xiao Luo [a], Shuyue Wang [a], Xiaopei Xu [a], Xiaocao Liu [a], Luwei Hong [a], Jixuan Li [a], Peiyu Huang [a], Minming Zhang [a,*], for the Alzheimer's Disease Neuroimaging Initiative[2]

[a] Department of Radiology, The Second Affiliated Hospital of Zhejiang University School of Medicine, Hangzhou, China
[b] Department of Radiology, Linyi People's Hospital, Linyi, China

ARTICLE INFO

Keywords:
Alzheimer's disease continuum
AT(N) classification system
Cognitively intact elderly
Basal forebrain cholinergic system
Functional connectivity

ABSTRACT

Background: A growing body of research reported the degeneration of the basal forebrain (BF) cholinergic system in the early course of Alzheimer's disease (AD). However, functional changes of the BF in asymptomatic individuals along the Alzheimer's continuum remain unclear.
Methods: A total of 229 cognitively intact participants were included from the Alzheimer's Disease Neuroimaging Initiative dataset and further divided into four groups based on the "A/T" profile using amyloid and tau positron emission tomography (PET). All A-T+ subjects were excluded. One hundred and seventy-three subjects along the Alzheimer's continuum (A-T-, A+ T-, A+ T+) were used for further study. The seed-based functional connectivity (FC) maps of the BF subregions (Ch1-3 and Ch4 [nucleus basalis of Meynert, NBM]) with whole-brain voxels were constructed. Analyses of covariance to detect the between-group differences and to further investigated the relations between FC values and AD biomarkers or cognition.
Results: We found increased FC between right Ch4 and bilateral amygdala among three groups, and the FC value could well distinguish between the A-T- group and the Alzheimer's continuum groups. Furthermore, increased FC between the Ch4 and amygdala was associated with higher pathological burden reflected by amyloid and tau PET in the entire population as well as better logistic memory function in A + T+ group.
Conclusion: Our study demonstrated the NBM functional connectivity increased in cognitively normal elderly along the Alzheimer's continuum, which indicated a potential compensatory mechanism to counteract pathological changes in AD and maintain intact cognitive function.

1. Introduction

Alzheimer's disease (AD) is described as a syndrome characterized by progressive and irreversible cognitive decline such as memory loss. However, AD pathological processes, including deposition of β-amyloid (Aβ) and formation of neurofibrillary tangles (NFTs), initiate years or even decades before clinical symptoms onset (Scheltens et al., 2016). Thus, a biological rather than a syndromal definition of AD would be more beneficial to understand its pathogenesis. Recently, Jack et al. (Jack et al., 2018) have proposed a novel research framework based on AD-related biomarkers: individuals with abnormal amyloid and tau biomarkers would be defined as biological AD. By applying this biological definition to research, asymptomatic individuals with existed AD pathological processes could be detected in the early stage and more accurate information for cerebral change could be obtained.

In neuropathological studies, degeneration of the cholinergic system in the basal forebrain (BF) is a specific feature of AD (Kása et al., 1997). Accumulating evidence suggests that neuronal damage and cell loss in

* Corresponding author at: Department of Radiology, Second Affiliated Hospital of Zhejiang University School of Medicine, No. 88 Jiefang Road, Shangcheng District, Hangzhou 310009, China.
E-mail address: zhangminming@zju.edu.cn (M. Zhang).

[1] Data used in preparation of this article were obtained from the Alzheimer's disease Neuroimaging Initiative (ADNI) database (http://www.loni.usc.edu). As such, the investigators within the ADNI contributed to the design and implementation of ADNI and/or provided data but did not participate in analysis or writing of this report. A complete listing of ADNI investigators can be found at: http://adni.loni.usc.edu/wpcontent/uploads/how_to _apply/ADNI_Acknowledgement_List.pdf.

[2] These authors have contributed equally to this work and share first authorship.

https://doi.org/10.1016/j.nicl.2022.103256
Received 7 June 2022; Received in revised form 16 October 2022; Accepted 31 October 2022
Available online 4 November 2022

the BF cholinergic system, most pronounced in the nucleus basalis of Meynert (NBM), occur in the preclinical and prodromal stages of AD, even before the deposition of neurofibrillary tangles (i.e., pre-tangle stages) (Chu et al., 2022; Grothe et al., 2012; Hanna Al-Shaikh et al., 2020). Magnetic resonance imaging (MRI) has emerged as a powerful in vivo technique to detect the structural and functional changes of BF. Whereas previous studies have reported atrophy of BF (Grothe et al., 2013; Grothe et al., 2012) and degeneration of the cholinergic white matter pathway (Nemy et al., 2020; Schumacher et al., 2021) at different clinical stages of AD, the functional changes of BF in asymptomatic individuals along the Alzheimer's continuum remain unclear.

In the present study, we aimed to investigate the seed-based functional connectivity (FC) of the BF in cognitively intact elderly along the Alzheimer's continuum. We hypothesized that FC alterations of the BF begin with the appearance of amyloid deposition and progress rapidly in individuals with both cerebral amyloidosis and tauopathy.

2. Materials and Methods

2.1. Study population

All data used in the current study were from the ADNI-3 database (https://adni.loni.usc.edu/). This ongoing project was launched in 2003 to develop clinical, neuropsychological, and neuroimaging biomarkers for early disease detection and progression monitoring of AD. The ADNI criteria for cognitively intact elderly were: 1) a Mini-Mental State Examination (MMSE) score of equal to or higher than 24 out of 30; 2) a Clinical Dementia Rating (CDR) score of 0; 3) and has no report of any cognition complaint.

In this study, we included 229 cognitively intact participants who fulfilled the following criteria before January 15th, 2021: 1) underwent resting-state functional MRI (fMRI) by 3.0 T MR scanner; 2) completed both amyloid positron emission tomography (PET) (^{18}F-florbetapir [AV-45] or ^{18}F-florbetaben [FBB]) and tau PET (^{18}F-flortaucipir [AV-1451]). Based on previously established cutoffs, amyloid positivity was defined by cortical-to-whole cerebellum standardized uptake value ratio (SUVR) $\geq$ 1.11 (for AV-45) (Landau et al., 2012) or $\geq$1.08 (for FBB) (Royse et al., 2021), and tau positivity was defined by Mayo's *meta*-ROI-to-cerebral crus 1 reference region $\geq$ 1.23 (Jack et al., 2017). Accordingly, we divided the study population into four groups: 1) A-T- (normal AD biomarkers, N = 105); 2) A + T- (Alzheimer's pathologic change, N = 35); 3) A + T+ (Alzheimer's disease, N = 45); and A-T+ (suspected non-Alzheimer's pathologic change [SNAP], N = 44). In line with Jack et al. (Jack et al., 2018), we defined A-T- as the reference group and A+ individuals (including A + T- and A + T +) as in the Alzheimer's continuum. All participants defined as SNAP were excluded. The study's flow chart is shown in Fig. 1.

2.2. Neuropsychological performance

All subjects underwent comprehensive neuropsychological examinations involving multiple cognition domains, including memory (Wechsler Memory Scale-Logical Memory [WMS-LM]), attention (trail-making test, Part A [TMT-A]), execution (trail-making test, Part B [TMT-B]), and language (animal fluency test [AFT]).

2.3. Image data acquisition

The resting-state fMRI images were obtained using an echo-planar imaging sequence with the following parameters: 197 time points; TR = 3000 ms; TE = 30 ms; slice thickness = 3.39 mm; spatial resolution = 3.39 × 3.39 × 3.39 mm^3; flip angle = 90o; and matrix = 64 × 64.

The structural MR images were obtained by using accelerated magnetization-prepared 180° radio-frequency pulses and rapid gradient-echo (MP-RAGE) sequence with the following parameters: TR = 2300 ms; TE = 3 ms; slice thickness = 1.0 mm; flip angle = 9.0°; and matrix = 256 × 256.

Amyloid PET imaging was undertaken using AV-45 or FBB, and tau PET was undertaken using AV-1451. Amyloid and tau PET images were acquired in 4 × 5-min frames and 6 × 5-min frames starting 50 and 75 min after intravenous bolus injection respectively. The detailed acquisition procedures were described in ADNI PET Technical Procedures Manual (http://adni.loni.usc.edu/wp-content/uploads/2012/10/ADNI3_PET-Tech Manual_V2.0_20161206.pdf).

2.4. BF regions of interest

The BF regions of interest (ROIs) were produced using the probabilistic atlases used by the SPM Anatomy Toolbox (https://www.fz-juelich.de/en/inm/inm-7/resources/jubrain-anatomy-toolbox/jubrain-toolbox) using previously published probabilistic maps of the BF (Zaborszky et al., 2008). According to Mesulam's nomenclature, the BF could be divided into 4 compartments: Ch1 corresponds to the medial septal nucleus, Ch2, and Ch3 to the vertical and horizontal limb of the diagonal band of Broca, and Ch4 refers to the cholinergic cells within the NBM (Mesulam et al., 1983). In reference to previous studies (Fernandez-Cabello et al., 2020; Nicolas et al., 2020), four ROIs were defined according to the stereotactic atlases as follows: (1) left and right medial septal nucleus and diagonal band of Broca (Ch1-3_L and Ch1-3_R); (2) left and right NBM (Ch4_L and Ch4_R).

2.5. Image data analysis

2.5.1. Resting-state fMRI analysis

The fMRI data were preprocessed by the Data Processing & Analysis

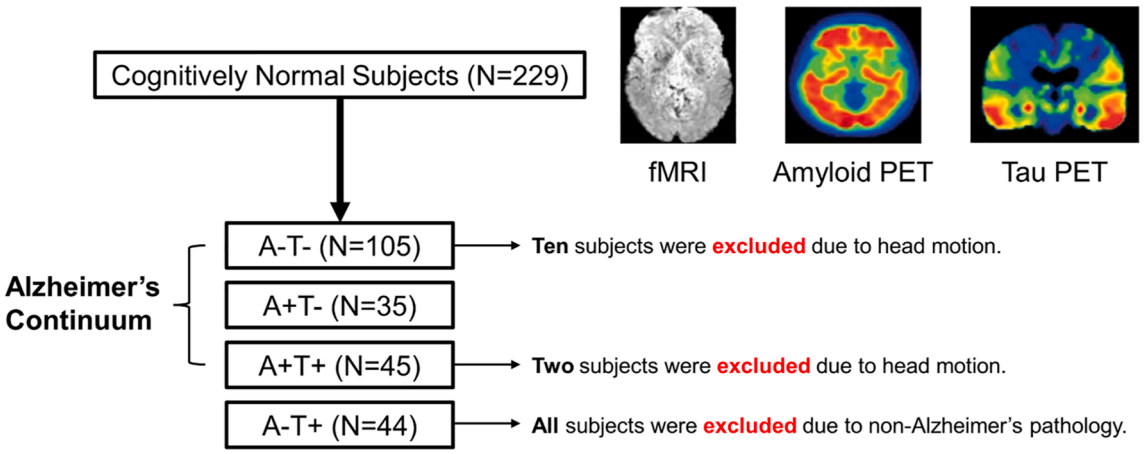

Fig. 1. Flow chart of participants inclusion from ADNI database.

for Brain Imaging (DPABI) toolbox (Yan et al., 2016) running under Statistical Parametric Mapping 12 (SPM12, https://www.fil.ion.ucl.ac.uk/spm/software/spm12/) software implemented in MATLAB (MathWorks, Natick). Firstly, the initial ten time points were discarded for the signal equilibrium and subject's adaptation. Then, the remaining images were corrected for slice time and head motion. We excluded 12 subjects (including 10 A-T- and 2 A + T + participants) according to the criteria of head motion more than 3.0 mm or 3.0° in maximum. After that, fMRI images were spatially normalized to the *EPI* template, resampled into 3 × 3 × 3 mm^3, and smoothed with a Gaussian kernel of 6 × 6 × 6 mm^3 full widths at half maximum to decrease spatial noise. Next, we removed linear trends and regressed out covariates, including Friston 24 head motion parameters, white matter signal, cerebrospinal fluid signal, and global signal. Finally, the fMRI images were band pass filtered to 0.01 and 0.1 Hz.

Individual seed-to-voxel FC map for each subject was calculated by the Dynamic Brain Connectome analysis toolbox (DynamicBC, http://restfmri.net/forum/DynamicBC) (Liao et al., 2014). Briefly, the FC maps were generated by calculating the Pearson coefficients between the time course of seed ROIs and remaining voxels. After that, the FC maps were transformed to zFC maps by Fisher's Z transformation for further statistical analysis.

2.5.1.1. Amyloid PET analysis. In this study, we used the results of AV-45 (UCBERKELEYAV45_05_12_20) and FBB (UCBERKELEYFBB_01_14_21) processed by UC Berkeley and Lawrence Berkeley National Laboratory. After co-registration to closest MR images, cortical-to-whole cerebellum summary SUVR was calculated by averaging across the 4 main cortical regions (frontal, anterior/posterior cingulate, lateral parietal, and lateral temporal cortex) dividing by the whole cerebellum (Landau et al., 2012).

2.5.1.2. Tau PET analysis. For the analysis of AV-1451, we used the processed results of Banner Alzheimer's Institute (BAI-PETNMRCFTP_03_03_20). Specifically, the AV-1451 PET images were co-registered to the closest MRI and then spatially normalized to template space using SPM12. Next, the composite SUVR value was computed as the median-uptake of voxels within the tau meta-ROI (entorhinal, amygdala, parahippocampal, fusiform, inferior temporal, and middle-temporal-ROIs) divided by the cerebellar-crus 1 region (Jack et al., 2017).

2.5.1.3. Structural MRI analysis. The structural MRI analysis was performed using the Computational Anatomy Toolbox 12 (CAT12, https://dbm.neuro.uni-jena.de/cat/) of SPM12. After applying the spatial adaptive non-local means (SANLM) denoising filter, the T1 images were segmented into gray matter (GM), white matter (WM), and cerebrospinal fluid partitions. Each mask of BF was deformed from MNI space to native space. Estimated volume of BF subregions were obtained by summing up the GM voxel values within the respective ROI masks as previous described (Fernandez-Cabello et al., 2020). The volumes of BF subregions were divided by the total intracranial volume (TIV) in order to correct for the effects of total brain size.

2.6. Statistical analysis

Statistical analyses of demographic data were performed using IBM SPSS Statistics Version 24 (IBM SPSS Statistics for Windows). Results with $p < 0.05$ were considered statistically significant. Continuous and categorical variables were expressed as mean ± standard deviation and percentage respectively. Image analyses of FC differences were conducted by DPABI toolbox. The effect of the group on FC of each basal forebrain subregions was assessed using analysis of covariance (ANCOVA), controlled for age, gender, and years of education. Comparison of FC maps was restricted to the gray matter areas and the Gaussian random field (GRF) method was applied to multiple comparisons correction. The statistical threshold was set at $p < 0.001$ with a cluster-level $p < 0.05$ (two-tailed). Considering the effect of apolipoprotein E (APOE) genotypes and head motion, we also repeated the analyses above after taking into APOE ε4 carrier status and mean framework displacement (FD) as covariates. For the reproducibility and generalizability of results, we performed the same analyses in the cohorts of individuals with MMSE total score ≥ 28.

The clusters with significant between-group differences were binarized to yield masks for extracting mean FC values from these clusters. Then, we performed a *post hoc* analysis between each group. The results were corrected for multiple comparisons by using the least significant difference (LSD) method. Furthermore, we performed the receiver operating characteristic (ROC) curves to investigate the classification performance of regional FC values. Specifically, we calculated the area under the curve (AUC) to distinguish the A-T- group from the A + T- group, the A + T + group, the Alzheimer's continuum groups (A + T- and A + T +), and the A + T- group from the A + T + group, respectively. Finally, to test the clinical significance, we also correlated the mean FC values from the clusters with neuropsychological performance and AD biomarkers by Pearson correlation analysis.

With respect to volumetric comparison of BF, we performed the ANCOVA among three groups after adjusting for age, sex, education, and TIV.

3. Results

3.1. Demographic and clinical characteristics

We included 95 A-T-, 35 A + T-, and 43 A + T + participants in the present study. Details regarding demographics and clinical characteristics are summarized in Table 1. There was no significant difference in gender distribution ($\chi^2 = 3.783$, $p = 0.151$), MMSE score ($F = 2.894$, $p = 0.058$), and education ($F = 0.157$, $p = 0.055$) among the three groups, while participants in A + T + group were older than the A-T- group ($p < 0.001$).

3.2. Between group differences in BF volume

There was no significant difference in BF sub-regional volume among the three groups (**Supplementary** Table 1**)**.

3.3. Between group differences in BF-FC

The FC of the bilateral Ch1-3 and Ch4_L did not differ significantly among the three groups, whereas FC between Ch4_R and bilateral amygdala showed significant difference (Fig. 2**,** Table 2). After post hoc analyses, we found an increasing trend of FC values among the three groups (Fig. 3). The averaged FC between right Ch4 with bilateral amygdala were listed in **Supplementary** Table 2. After controlling for head motion or both APOE ε4 carrier status and head motion, the results remain unchanged (**Supplementary** Figs. 1, 2). Moreover, we found similar results in cohort of individuals with MMSE total score ≥ 28 (**Supplementary Figure 3, 4, 5**).

Table 3 shows the AUC values of FC between Ch4_R and left/right amygdala in A-T- vs A + T- (0.558; 0.600), A-T- vs A + T+ (0.699; 0.626), A + T- vs A + T+ (0.621; 0.546), A-T- vs A + T- and A + T+ (0.636; 0.614) classifications.

3.4. Correlations between FC with neuropsychological tests and AD biomarkers

In the overall sample, the FC between Ch4_R and left amygdala (Ch4_R_Amygdala_L FC) was associated with tau PET temporal *meta*-ROIs SUVR ($r = 0.227$, $p = 0.003$). The FC between Ch4_R and right amygdala (Ch4_R_Amygdala_R FC) was related to both Aβ PET summary

Table 1
Demographics, neuropsychological performance, amyloid and tau PET of the three groups.

Variables	A-T- group (N = 95)	A + T- group (N = 35)	A + T + group (N = 43)	F/χ^2	*p* value
Age	69.94 ± 6.74	73.07 ± 7.98	75.19 ± 6.32[a]	9.198	<0.001
Gender (M/F)	30/65	13/22	21/22	3.783	0.151
Education	16.63 ± 2.18	16.80 ± 2.39	16.84 ± 2.18	0.157	0.855
MMSE	29.26 ± 0.95	29.00 ± 1.08	28.74 ± 1.68	2.894	0.058
WMS-LM immediate recall	14.62 ± 3.41	15.11 ± 3.24	13.67 ± 3.81	1.802	0.168
WMS-LM delayed recall	13.55 ± 3.49	14.43 ± 3.07	12.47 ± 3.65[b]	3.194	0.044
TMT-A	29.87 ± 9.23	30.86 ± 9.25	31.79 ± 9.70	0.646	0.525
TMT-B	66.52 ± 31.44	75.54 ± 47.07	85.19 ± 50.17[a]	3.291	0.040
AFT	22.68 ± 5.46	21.60 ± 5.23	21.00 ± 5.51	1.574	0.210
Amyloid PET	5.67 ± 9.06	53.65 ± 27.07[a]	59.73 ± 34.56[a]	116.584	<0.001
Tau PET	1.15 ± 0.06	1.17 ± 0.06	1.35 ± 0.15[ab]	73.538	<0.001

Notes: Data are presented as means ± standard deviations.
Abbreviation: MMSE, Mini Mental State Examination; WMS-LM, Wechsler Memory Scale-Logical Memory; TMT-A, Trail Making Test Part A; TMT-B, Trail Making Test Part B; AFT, Animal fluency test; PET, Positron Emission Tomography.
[a] compared to A-T- group, $p < 0.05$, LSD corrected.
[b] compared to A + T- group, $p < 0.05$, LSD corrected.

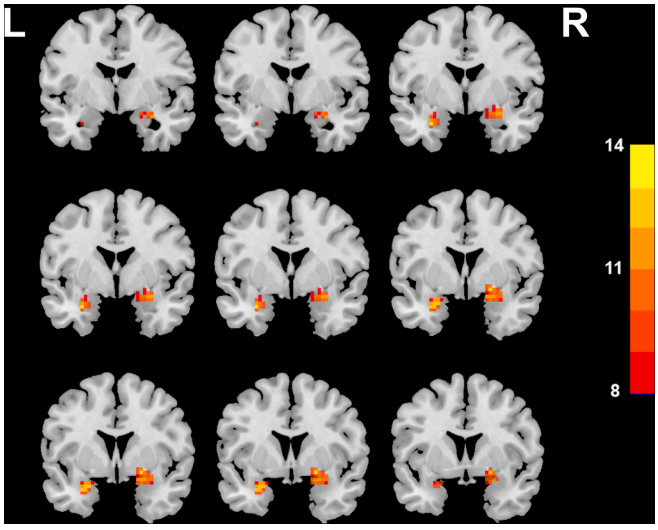

Fig. 2. The ANCOVA analysis showed that FC between right NBM (i.e., Ch4) and bilateral amygdala showed significant difference among three groups after controlling for age, gender, and education ($p < 0.001$ with a cluster level $p < 0.05$, two-tailed, GRF corrected). Abbreviations ANCOVA, analysis of covariance FC, functional connectivity NBM, nucleus basalis of MeynertGRF, gaussian random field.

SUVR ($r = 0.183$, $p = 0.016$) and tau PET temporal *meta*-ROIs SUVR ($r = 0.186$, $p = 0.014$) (Table 4, **Supplementary Figure 6**). The results using partial correlation analysis were shown in **Supplementary** Table 3.

In A + T + cohort, Ch4_R_Amygdala_R FC was associated WMS-Logistic memory immediate recall ($r = 0.316$, $p = 0.039$) and delayed recall ($r = 0.362$, $p = 0.017$) (Table 5). However, in Alzheimer's continuum (A + T- and A + T + groups), No significant association was established between FC of Ch4_R with bilateral amygdala and cognitive function or AD biomarkers **(Supplementary** Table 4**)**.

Table 2
Brain areas showing between-group differences on FC of right Ch4.

Brain region	Number of voxels	Peak MNI coordinate			Peak intensity
		X	Y	Z	
Left amygdala	28	−30	0	−24	13.902
Right amygdala	65	21	3	−9	14.480

Notes: The statistical threshold was set at $p < 0.001$ with a cluster level $p < 0.05$ (two-tailed, GRF corrected).
Abbreviation: FC, functional connectivity; MNI, Montreal Neurological Institute; GRF, gaussian random field.

4. Discussion

In this study, we assessed the alteration of functional change in BF measured by resting-state fMRI in the cognitively intact individuals with the existed pathological processes. Notably, we observed increasing FC between right NBM and bilateral amygdala with the progression of AD pathology. Furthermore, NBM-FC was positively correlated with cerebral amyloidosis, tauopathy, and memory function. Our findings suggested that NBM functional change occurred and increased in cognitively normal elders along the Alzheimer's continuum, which indicated a potential compensatory mechanism to counteract AD pathology and maintain intact cognitive function.

Our results of NBM functional alteration in the early preclinical stage demonstrated its vulnerability to AD pathology. The NBM (i.e., Ch4) is the largest of the four cholinergic nuclei of the BF (Mesulam et al., 1983), measuring 13–14 mm antero-posteriorly and 16–18 mm mediolaterally (Mesulam and Geula, 1988). As we expected, FC alteration of the NBM begins with the appearance of amyloid deposition. Evidence from systematic reviews shows a strong relationship between amyloid deposition and brain cholinergic dysfunction in the NBM (Hampel et al., 2018; Majdi et al., 2020; Pákáski and Kálmán, 2008). By combining amyloid PET and structural MRI, some studies have reported that BF atrophy is closely related to cortical Aβ burden in pre-symptomatic and predementia stages of AD (Grothe et al., 2014; Teipel et al., 2014; Yoo et al., 2022). Based on resting-state fMRI, a significant in vivo association between BF dynamics and global Aβ accumulation was observed in cognitively intact older adults with subjective memory complaints (Chiesa et al., 2019). In addition to Aβ deposition, a massive load of NFTs could also be traced in the NBM during the early course of the disease (Mesulam et al., 2004). Significantly, concurrent Aβ deposition and NFTs formation could induce serious neuron degeneration of the BF cholinergic system (Majdi et al., 2020). Therefore, our finding of a rapid change in FC of the NBM in individuals with both amyloidosis and tauopathy suggests that the interaction of these two pathologies can accelerate the functional changes of NBM.

Furthermore, we found that the NBM shows a specific functional connection with the amygdala. Anatomically, the amygdala is also the target region that receives the major sources of cholinergic innervation from the NBM (Blake and Boccia, 2018; Mesulam and Geula, 1988). In cognitively intact elderly people, atrophy of the amygdala on MRI occurs 10 years before the onset of clinical symptoms in AD and could predict the onset of dementia (den Heijer et al., 2006; Tondelli et al., 2012). Also, atrophy of the amygdala showed a significant association with volume loss of NBM in the preclinical phase (A + T+, asymptomatic) of AD (Cantero et al., 2020). Taken together, the connection between the NBM and amygdala may be an important target for exploring the early cerebral changes of AD. Interestingly, we only found the between-group differences in FC of right NBM, which may indicate the hemispheric asymmetric features of cholinergic system. Both postmortem and in-vivo studies have observed the pronounce atrophy of right NBM in MCI and AD (Teipel et al., 2005; Teipel et al., 2011). Thus,

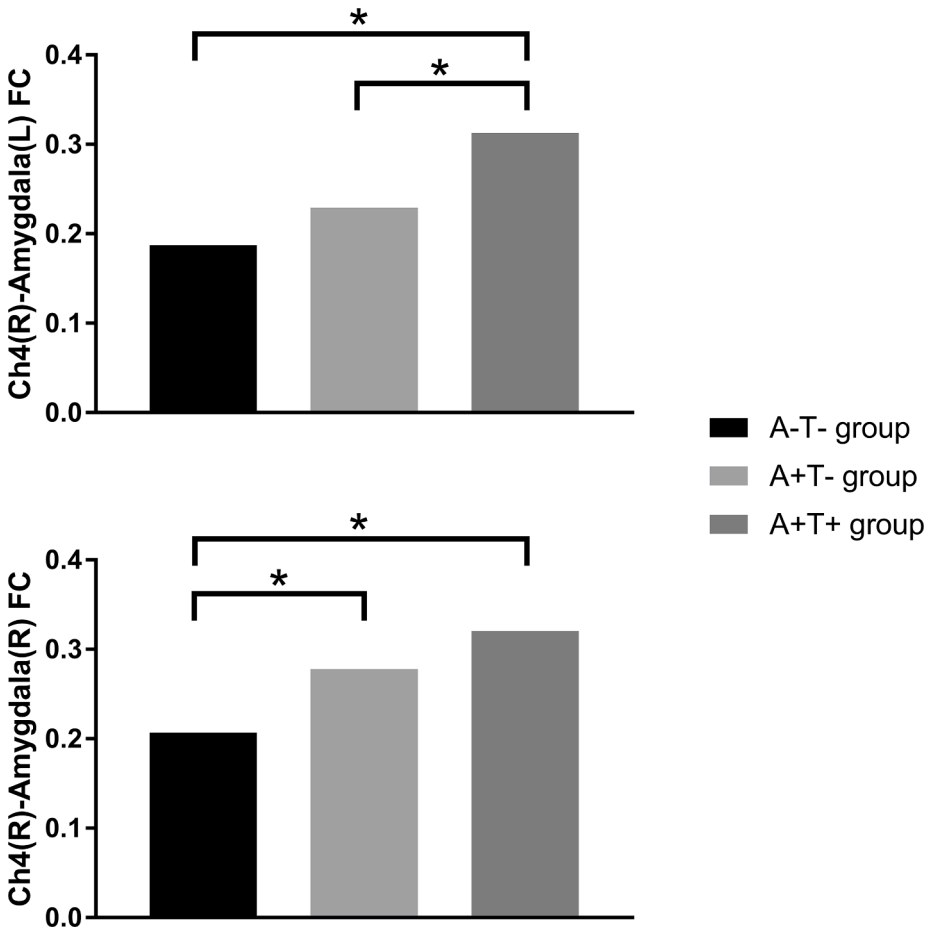

Fig. 3. A post hoc-test of main effect for group. Significant differences are marked by asterisks as shown: * represents significance level of $p < 0.05$. Abbreviations: FC, functional connectivity.

Table 3
The AUC values of classification performance.

Group classifications	Ch4_R_Amygdala_L	Ch4_R_Amygdala_R
A-T- group vs A + T- group	0.558	0.558
A-T- group vs A + T + group	0.699	0.699
A + T- group vs A + T + group	0.621	0.621
A-T- group vs A + T- and A + T + groups	0.636	0.636

Abbreviation: AUC, area under the curve; L, left; R, right.

we speculated that the right NBM might be more vulnerable to Alzheimer's pathology than the left.

Furthermore, we observed that the FC between NBM and amygdala continuously increased in asymptomatic individuals along the Alzheimer's continuum. Our findings are consistent with a previous work which found increased connectivity or cerebral blood flow (CBF) in individuals at high risk for AD who have not yet been considered cognitively impaired. For example, increased FC of the NBM with the supplementary motor area was observed in subjective cognitive decline (SCD) compared to healthy controls based on resting-state fMRI (Xu et al., 2021). Using arterial spin labeling (ASL) MRI, Fazlollahi et al. (Fazlollahi et al., 2020) observed a positive correlation between CBF and Aβ burden in the amygdala in cognitively normal subjects with a positive Aβ burden. Additionally, the FC value between the NBM and amygdala could well distinguish between the A-T- group and the Alzheimer's continuum groups, indicating that it could be an early neuroimaging classification biomarker. Furthermore, FC between NBM and amygdala in this study showed significant positive correlations with AD

Table 4
Associations between right Ch4 to bilateral amygdala FC with cognitive function and AD biomarkers in whole sample.

	Ch4_R_Amygdala_L		Ch4_R_Amygdala_R	
	r	*p*	r	*p*
Cognitive function				
MMSE	0.095	0.214	0.034	0.653
WMS-LM immediate recall	−0.027	0.730	0.067	0.383
WMS-LM delayed recall	−0.015	0.849	0.085	0.269
TMT-A	0.000	0.998	0.067	0.388
TMT-B	−0.041	0.595	0.057	0.453
AFT	−0.081	0.291	0.036	0.637
AD biomarkers				
Aβ PET summary SUVR	0.095	0.211	0.183	**0.016***
Tau PET SUVR (Temporal meta-ROIs)	0.227	**0.003***	0.186	**0.014***

* $p < 0.05$.
Abbreviation: FC, functional connectivity; AD, Alzheimer's disease; MMSE, Mini Mental State Examination; WMS-LM, Wechsler Memory Scale-Logical Memory; TMT-A, Trail Making Test Part A; TMT-B, Trail Making Test Part B; AFT, Animal fluency test; PET, Positron Emission Tomography; SUVR, standardized uptake value ratio; ROI, regions of interest; L, left; R, right.

pathologies and memory function. Amygdala is a component of the limbic system and plays a fundamental role in emotion mediation and memory function (LaBar and Cabeza, 2006; LeDoux, 2007). Numerous studies based on tau PET have highlighted that the amygdala is also one of the key regions susceptible to tau pathology in the early stage of AD (Cho et al., 2016; Leuzy et al., 2022; Schwarz et al., 2016). Considering no significant cognitive impairment has been found in our study

Table 5
Associations between right Ch4 to bilateral amygdala FC with cognitive function and AD biomarkers in A + T + cohort.

	Ch4_R_Amygdala_L		Ch4_R_Amygdala_R	
	r	*p*	r	*p*
Cognitive function				
MMSE	0.129	0.408	0.172	0.269
WMS-LM immediate recall	−0.042	0.791	0.316	**0.039***
WMS-LM delayed recall	−0.011	0.943	0.362	**0.017***
TMT-A	−0.059	0.706	−0.125	0.426
TMT-B	−0.059	0.705	−0.138	0.378
AFT	−0.177	0.255	0.094	0.549
AD biomarkers				
Aβ PET summary SUVR	−0.113	0.471	−0.063	0.688
Tau PET SUVR (Temporal meta-ROIs)	0.121	0.438	0.087	0.577

* $p < 0.05$.
Abbreviation: FC, functional connectivity; AD, Alzheimer's disease; MMSE, Mini Mental State Examination; WMS-LM, Wechsler Memory Scale-Logical Memory; TMT-A, Trail Making Test Part A; TMT-B, Trail Making Test Part B; AFT, Animal fluency test; PET, Positron Emission Tomography; SUVR, standardized uptake value ratio; ROI, regions of interest; L, left; R, right.

population, we hypothesized that increasing FC we observed would be a potential compensative mechanism that protects the brain from different pathologies and maintains the intact cognitive function in the early stage of AD.

However, we did not find significant differences in FC of the Ch1-3 subregion among the three groups Anatomically, Ch12 mainly innervates hippocampal structures, while Ch3 innervates the olfactory bulb (Blake and Boccia, 2018; Mesulam et al., 1983). In MCI due to AD, atrophy was most pronounced in the posterior NBM, sparing the Ch12 area (Grothe et al., 2010; Richter et al., 2022). In addition, in vivo MRI evidence supports the idea that abnormally phosphorylated tau is selectively associated with atrophy of the NBM in asymptomatic subjects at risk for AD, which then spreads to the Ch12 in both preclinical and prodromal AD (Cantero et al., 2020). Moreover, it is well known that memory loss, amyloidosis, and tauopathy were significant in the profound degeneration of the NBM. Therefore, we hypothesize that the degeneration first occurs in NBM, and then with the progression of disease, occurs in Ch1-3 occurs as well. Nevertheless, it is noteworthy that our findings are derived from a cross-sectional study and therefore it prevents us from inferring the time course of these changes. Future longitudinal studies can follow the time course of the functional changes in the BF cholinergic system to make inferences about the trajectory of the disease.

There are still several limitations to the study. First, the sample size for FC analyses was relatively small. Future studies would require a larger sample size to validate our findings. Second, this study lacks longitudinal follow-up data. Performing a longitudinal comparison, especially in subjects with biomarker profile A-T- to A + T- or A + T- to A + T+, could reveal the earliest difference in the Alzheimer's continuum. Finally, the present study focused only on functional changes in BF using fMRI, and exploring cholinergic white matter pathways in the Alzheimer's continuum will be of particular interest in future studies.

5. Conclusions

To sum up, our results showed increased FC between NBM and amygdala in cognitively intact elderly along the Alzheimer's continuum, suggesting that functional alteration of the BF cholinergic system begins in an early stage of AD and NBM-to-amygdala FC may be a compensatory response to AD pathology.

Ethical approvals

All procedures performed in studies involving human participants were in accordance with the ethical standards of the institutional and/or national research committee and with the 1964 Helsinki declaration and its later amendments or comparable ethical standards.

CRediT authorship contribution statement

Qingze Zeng: Conceptualization, Writing – original draft. **Tiantian Qiu:** Conceptualization, Writing – original draft. **Kaicheng Li:** Conceptualization, Writing – original draft. **Xiao Luo:** Formal analysis, Funding acquisition. **Shuyue Wang:** Resources. **Xiaopei Xu:** Writing – review & editing. **Xiaocao Liu:** Visualization. **Luwei Hong:** Software. **Jixuan Li:** Writing – review & editing. **Peiyu Huang:** Writing – review & editing. **Minming Zhang:** Methodology, Writing – review & editing.

Declaration of Competing Interest

The authors declare that they have no known competing financial interests or personal relationships that could have appeared to influence the work reported in this paper.

Data availability

The data used in the preparation of this article were obtained from the Alzheimer's disease Neuroimaging Initiative (ADNI) database: https://adni.loni.usc.edu/.

Acknowledgements

This study was funded by the National Natural Science Foundation of China (Grant No. 81901707 and 82001766), Linyi Science and Technology Development Program (Grant No. 202020024), and Shandong Medicine and Health Science and Technology Program (Grant No. 202009010844). The data collection and sharing for this project were funded by the ADNI (National Institutes of Health Grant U01 AG024904) and DOD ADNI (Department of Defense Award No. W81XWH-12-2-0012).

Consent to participate

Written informed consent was obtained from all participants and/or authorized representatives and the study partners before any protocol-specific procedures were carried out in the ADNI study.

References

Blake, M.G., Boccia, M.M., 2018. Basal forebrain cholinergic system and memory. Curr. Top Behav. Neurosci. 37, 253–273.
Cantero, J.L., et al., 2020. Atrophy of basal forebrain initiates with tau pathology in individuals at risk for Alzheimer's disease. Cereb. Cortex 30, 2083–2098.
Chiesa, P.A., et al., 2019. Relationship between basal forebrain resting-state functional connectivity and brain amyloid-beta deposition in cognitively intact older adults with subjective memory complaints. Radiology 290, 167–176.
Cho, H., et al., 2016. In vivo cortical spreading pattern of tau and amyloid in the Alzheimer disease spectrum. Ann. Neurol. 80, 247–258.
Chu, W.T., et al., 2022. Association of cognitive impairment with free water in the nucleus basalis of meynert and locus coeruleus to transentorhinal cortex tract. Neurology. 98, e700–e710.
den Heijer, T., et al., 2006. Use of hippocampal and amygdalar volumes on magnetic resonance imaging to predict dementia in cognitively intact elderly people. Arch. Gen. Psychiatry 63, 57–62.
Fazlollahi, A., et al., 2020. Increased cerebral blood flow with increased amyloid burden in the preclinical phase of alzheimer's disease. J. Magn. Reson. Imaging 51, 505–513.
Fernandez-Cabello, S., et al., 2020. Basal forebrain volume reliably predicts the cortical spread of Alzheimer's degeneration. Brain. 143, 993–1009.
Grothe, M., et al., 2010. Reduction of basal forebrain cholinergic system parallels cognitive impairment in patients at high risk of developing Alzheimer's disease. Cereb. Cortex 20, 1685–1695.
Grothe, M., et al., 2012. Atrophy of the cholinergic Basal forebrain over the adult age range and in early stages of Alzheimer's disease. Biol. Psychiatry 71, 805–813.

Grothe, M., et al., 2013. Longitudinal measures of cholinergic forebrain atrophy in the transition from healthy aging to Alzheimer's disease. Neurobiol. Aging 34, 1210–1220.
Grothe, M.J., et al., 2014. Basal forebrain atrophy and cortical amyloid deposition in nondemented elderly subjects. Alzheimers Dement. 10, S344–S353.
Hampel, H., et al., 2018. The cholinergic system in the pathophysiology and treatment of Alzheimer's disease. Brain. 141, 1917–1933.
Hanna Al-Shaikh, F.S., et al., 2020. Selective vulnerability of the nucleus Basalis of Meynert among neuropathologic subtypes of Alzheimer disease. JAMA Neurol. 77, 225–233.
Jack Jr, C.R., et al., 2017. Defining imaging biomarker cut points for brain aging and Alzheimer's disease. Alzheimers Dement. 13, 205–216.
Jack Jr, C.R., et al., 2018. NIA-AA research framework: Toward a biological definition of Alzheimer's disease. Alzheimers Dement. 14, 535–562.
Kása, P., et al., 1997. The cholinergic system in Alzheimer's disease. Prog. Neurobiol. 52, 511–535.
LaBar, K.S., Cabeza, R., 2006. Cognitive neuroscience of emotional memory. Nat. Rev. Neurosci. 7, 54–64.
Landau, S.M., et al., 2012. Amyloid deposition, hypometabolism, and longitudinal cognitive decline. Ann. Neurol. 72, 578–586.
LeDoux, J., 2007. The amygdala. Curr. Biol. 17, R868–R874.
Leuzy, A., et al., 2022. Biomarker-based prediction of longitudinal tau positron emission tomography in Alzheimer disease. JAMA Neurol. 79, 149–158.
Liao, W., et al., 2014. DynamicBC: a MATLAB toolbox for dynamic brain connectome analysis. Brain Connect. 4, 780–790.
Majdi, A., et al., 2020. Amyloid-β, tau, and the cholinergic system in Alzheimer's disease: seeking direction in a tangle of clues. Rev. Neurosci. 31, 391–413.
Mesulam, M.M., et al., 1983. Cholinergic innervation of cortex by the basal forebrain: cytochemistry and cortical connections of the septal area, diagonal band nuclei, nucleus basalis (substantia innominata), and hypothalamus in the rhesus monkey. J. Comp. Neurol. 214, 170–197.
Mesulam, M., et al., 2004. Cholinergic nucleus basalis tauopathy emerges early in the aging-MCI-AD continuum. Ann. Neurol. 55, 815–828.
Mesulam, M.M., Geula, C., 1988. Nucleus basalis (Ch4) and cortical cholinergic innervation in the human brain: observations based on the distribution of acetylcholinesterase and choline acetyltransferase. J. Comp. Neurol. 275, 216–240.
Nemy, M., et al., 2020. Cholinergic white matter pathways make a stronger contribution to attention and memory in normal aging than cerebrovascular health and nucleus basalis of Meynert. Neuroimage. 211, 116607.
Nicolas, B., et al., 2020. Basal forebrain metabolism in Alzheimer's disease continuum: relationship with education. Neurobiol. Aging 87, 70–77.
Pákáski, M., Kálmán, J., 2008. Interactions between the amyloid and cholinergic mechanisms in Alzheimer's disease. Neurochem. Int. 53, 103–111.
Richter, N., et al., 2022. Age and anterior basal forebrain volume predict the cholinergic deficit in patients with mild cognitive impairment due to Alzheimer's Disease. J. Alzheimers Dis. 86, 425–440.
Royse, S.K., et al., 2021. Validation of amyloid PET positivity thresholds in centiloids: a multisite PET study approach. Alzheimers Res Ther. 13, 99.
Scheltens, P., et al., 2016. Alzheimer's disease. Lancet 388, 505–517.
Schumacher, J., et al., 2021. Cholinergic white matter pathways in dementia with Lewy bodies and Alzheimer's disease. Brain.
Schwarz, A.J., et al., 2016. Regional profiles of the candidate tau PET ligand 18F-AV-1451 recapitulate key features of Braak histopathological stages. Brain. 139, 1539–1550.
Teipel, S.J., et al., 2005. Measurement of basal forebrain atrophy in Alzheimer's disease using MRI. Brain 128, 2626–2644.
Teipel, S.J., et al., 2011. The cholinergic system in mild cognitive impairment and Alzheimer's disease: an in vivo MRI and DTI study. Hum. Brain Mapp. 32, 1349–1362.
Teipel, S., et al., 2014. Cholinergic basal forebrain atrophy predicts amyloid burden in Alzheimer's disease. Neurobiol. Aging 35, 482–491.
Tondelli, M., et al., 2012. Structural MRI changes detectable up to ten years before clinical Alzheimer's disease. Neurobiol Aging. 33, 825.e25–825.e36.
Xu, W., et al., 2021. Altered functional connectivity of the basal nucleus of meynert in subjective cognitive impairment, early mild cognitive impairment, and late mild cognitive impairment. Front. Aging Neurosci. 13, 671351.
Yan, C.G., et al., 2016. DPABI: data processing & analysis for (resting-state) brain imaging. Neuroinformatics. 14, 339–351.
Yoo, H.S., et al., 2022. Association of β-amyloid and basal forebrain with cortical thickness and cognition in alzheimer and Lewy body disease spectra. Neurology. 98, e947–e957.
Zaborszky, L., et al., 2008. Stereotaxic probabilistic maps of the magnocellular cell groups in human basal forebrain. Neuroimage. 42, 1127–1141.